Discovery of Highly Isoform Selective Orally Bioavailable Phosphoinositide 3-Kinase (PI3K)-γ Inhibitors

Nils Pemberton,*,† Mickael Mogemark,*,‡ Susanne Arlbrandt,† Peter Bold,† Rhona J. Cox,† Cristina Gardelli,† Neil S. Holden,†,# Kostas Karabelas,†,∇ Johan Karlsson,§,○ Sarah Lever,† Xueshan Li,‖ Helena Lindmark,§ Monica Norberg,† Matthew W. D. Perry,† Jens Petersen,§ Sandra Rodrigo Blomqvist,† Matthew Thomas,†,◆ Christian Tyrchan,† Annika Westin Eriksson,‡ Pavol Zlatoidsky,† and Linda Öster§

†Respiratory, Inflammation & Autoimmunity, ‡Drug Safety and Metabolism, and §Discovery Sciences, IMED Biotech Unit, AstraZeneca Gothenburg, SE-43183 Mölndal, Sweden

‖Pharmaron Beijing Co., Ltd., No. 6 Taihe Road, BDA, Beijing 100176, P. R. China

S Supporting Information

ABSTRACT: In this paper, we describe the discovery and optimization of a new chemotype of isoform selective PI3Kγ inhibitors. Starting from an HTS hit, potency and physicochemical properties could be improved to give compounds such as **15**, which is a potent and remarkably selective PI3Kγ inhibitor with ADME properties suitable for oral administration. Compound **15** was advanced into in vivo studies showing dose-dependent inhibition of LPS-induced airway neutrophilia in rats when administered orally.

15

Enz. pIC$_{50}$ α: 5.1, β: <4.5, γ: 9.1, δ: 6.5
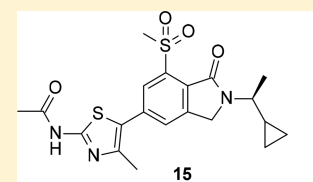
Cell pIC$_{50}$ α: <4.5, β: <4.5, γ: 8.1, δ: 6.0

INTRODUCTION

Phosphoinositide 3-kinases (PI3Ks) are lipid kinases whose primary function is to catalyze phosphorylation of the 3-position of the inositol ring of membrane phosphoinositides. This initiates a complex downstream signaling network that regulates cell growth, survival, migration, and proliferation. The PI3K family is clustered into three different classes (classes I, II, and III) based on structural features and substrate preference. Class I consists of four isoforms (α, β, γ, and δ). It is by far the most extensively studied of the PI3K classes and has been an attractive target for the pharmaceutical industry over the past decade. The PI3Kγ isoform is primarily found in leukocytes and is a key regulator of cellular migration.[1,2] A PI3Kγ inhibitor could thus potentially be used to treat a variety of diseases in which influx of inflammatory effector cells plays a key role in pathology, including diseases within the areas of respiratory and inflammation, metabolic disorders, and cancer.[3−5] Unfortunately, highly selective PI3Kγ inhibitors are rare as it has been difficult to identify truly isoenzyme selective compounds due to the high sequence homology between the PI3K isoforms. From a safety perspective, high isoform selectivity is essential as PI3Kα has been shown to affect glucose and insulin signaling.[6] It has also been shown that PI3Kγ knockout mice are viable and fertile while genetic inactivation of PI3Kα or -β results in embryonic lethality.[7,8] Recently compounds with high γ isoform selectivity have been reported, including IPI-549 which is currently in clinical trials in immuno-oncology applications.[9−11] We now report our discovery of a series of highly selective PI3Kγ inhibitors. This series, which was identified in a HTS, contains an isoindolinone core that extends deep into the ATP-binding pocket and utilizes a selectivity switch that has not been previously described for PI3K inhibitors.

RESULTS AND DISCUSSION

Our efforts to discover selective PI3Kγ inhibitors with suitable ADME properties for oral dosing started with a full HTS of our corporate screening collection using a biochemical enzyme inhibition assay for PI3Kγ. This was followed by a counter-screen for PI3Kα in order to identify series with some inherent PI3Kγ selectivity. One hit series contained an isoindolinone core (Figure 1). Compound **1** was one of the most potent in this cluster and exhibited high selectivity toward PI3Kα. It was
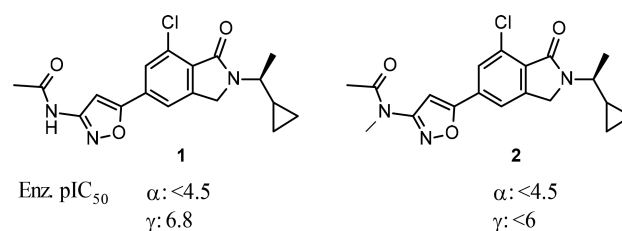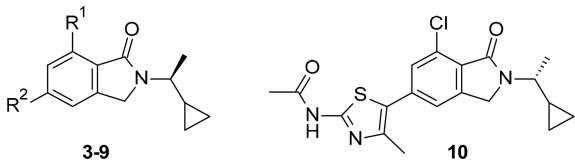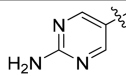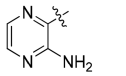

Enz. pIC$_{50}$

1 α: <4.5, γ: 6.8

2 α: <4.5, γ: <6
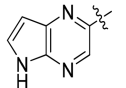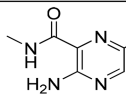
Figure 1. Isoindolinone containing HTS hit **1** identified as an inhibitor of PI3Kγ and methylated analogue **2**.

Table 1. Structure, PI3K Enzyme and Cell Inhibitory Potencies, and Pharmacokinetically Relevant Properties of Compounds 3−10[a]

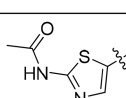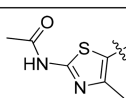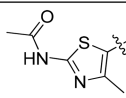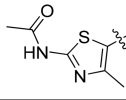| Compd	R^1	R^2	PI3Kγ enz. pIC_{50}	PI3Kα enz. pIC_{50}	PI3Kβ enz. pIC_{50}	PI3Kδ enz. pIC_{50}	PI3Kγ cell pIC_{50}	logD, pH 7.4	Sol., pH 7.4 (μM)	Rat CL_{int}[d]
3	Cl		8.0	<4.5	<4.5	NT[c]	6.2	2.6	5	2
4	Me		7.6	<4.5[‡]	<4.5[†]	5.0[†]	5.1[†]	2.6	117	43
5	Me		8.2	4.6[‡]	<4.5[‡]	5.2[‡]	6.4[†]	4.3	7	146
6	Me		8.1[‡]	5.2[†]	<4.5[‡]	5.5[‡]	6.4	3.8	8	4
7	Cl		8.9[‡]	5.0	<4.5	5.8	7.5	3.8	3	2
8	Cl		9.1	5.6	5.0	6.5	8.2	3.9	1	3
9	Me		9.2	5.5	4.7	6.7	8.2	4.3	1	11
10[b]	Cl		8.9	5.6	4.8	6.3	7.4	3.9	13	6

[a]All biological values are the mean of ≥3 replicates except [‡]$n = 2$, [†]$n = 1$. [b]Compound **10**, which is also depicted above, is the *R*-enantiomer. [c]NT, not tested. [d]Intrinsic clearance in rat hepatocytes ((μL/min)/10^6 cells).

profiled in a PI3Kγ target engagement cell assay measuring phosphorylation of AKT but was inactive at 1 μM.[12]

The attractive selectivity profile meant that this series was still deemed to be of interest. It was not immediately apparent what binding mode the compounds might have in the PI3Kγ enzyme, and we made repeated efforts to crystallize compounds from this series with a PI3Kγ construct to guide further design but without success. This was surprising since PI3Kγ has been shown to be very amenable to crystallization and has often been used as a surrogate for the other class 1 PI3Ks;[13] at AstraZeneca our in-house database contains more than 80 PI3Kγ structures. We screened near neighbors of **1** to build a picture of the SAR. Compound **2**, a methylated matched-pair analogue of **1**, lost significant PI3Kγ activity (Figure 1). This prompted us to hypothesize that the acetamido-substituted isoxazole might interact with the hinge region of the kinase. Even though isoxazole is not a common hinge-binding motif, it does contain a hydrogen bond donor/acceptor pair typical for

kinase inhibitors. The dependence of activity on the donor NH suggested this could be a good place to start exploring SAR.

A set of amino heterocycles that are typical kinase hinge-binding motifs were therefore introduced to replace the isoxazole (Table 1). Encouragingly, several of these such as aminopyrimidine **3** and pyrrolopyrazine **5** were potent inhibitors of PI3Kγ, supporting the hypothesis that this part of the molecule was interacting with the hinge. This was further strengthened with data for compounds **6−10** which all carried hinge-binding motifs that had been used in previously reported PI3Kγ inhibitors.[6,14,15] The introduction of an aminothiazole heterocycle in **7−10** gave a marked increase in enzyme potency, and to our delight this was also reflected in the data from the cell assay showing pIC_{50} of **7−8** (Table 1). These results clearly supported the hypothesis that this part of the molecule was binding to the hinge region, but we were still unable to crystallize these more potent compounds in our PI3Kγ construct.

Compounds **3−10** all showed very good selectivity toward the other class I isoforms. Compound **9**, however, was a moderately potent inhibitor of PI3Kδ, and we therefore investigated crystallization in a PI3Kδ construct. Rewardingly, this was successful, and crystals of **9** in mouse PI3Kδ could be obtained (Figure 2). The structure confirms that the amino-
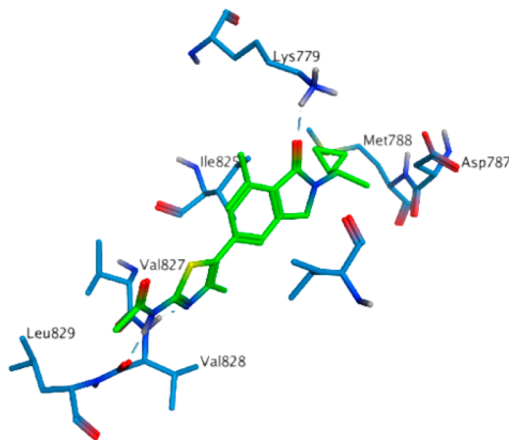

Figure 2. X-ray crystal structure of compound **9** in mouse PI3Kδ (PDB code 6FTN). The aminothiazole forms hydrogen bonds to the hinge residue Val828. The carbonyl of the lactam interacts with Lys779. The N-alkyl tail is oriented perpendicular to the isoindolinone core and is extending deep into the ATP-binding pocket.

thiazole heterocycle is interacting with the hinge residues as bidentate hydrogen bonds to Val828 are observed. The isoindolinone core forms hydrophobic interactions with Ile825 and the carbonyl of the lactam hydrogen-bonds with the catalytic Lys779. All these interactions are made with residues that are conserved between all four isoforms and do not give any clue to the high isoform selectivity observed in this series. However, one feature that is unique in this series is the N-alkyl tail, which is oriented perpendicular to the isoindolinone core, positioning the cyclopropyl ring close to Met788 and the methyl close to Asp787, both residues that form part of the kα3-helix (the equivalent to αC-helix in protein kinases). This observation prompted further investigation of the N-alkyl substituent, and a set of analogues was prepared. However, out of the 80 compounds prepared in this set no compound had increased potency compared to the original methylcyclopropyl moiety that originated from the HTS hit (data not shown). The stereochemistry did not have a large impact on selectivity or potency as the (R)-stereoisomer **10** had similar potency in the biochemical assay to the (S)-stereoisomer **8** but was slightly less potent in the cell assay (Table 1). More interesting results were obtained when removing the alkyl group from the nitrogen altogether giving compound **11** (Table 2).

Comparison of the matched-pair analogues **9** and **11** showed a dramatic 2 log drop in PI3Kγ potency, while PI3Kα potency increased by 1.6 log. Interestingly, PI3Kδ potency was hardly affected and PI3Kβ potency increased but less dramatically than α. The remarkable PI3Kγ selectivity thus seems to originate from the N-alkyl tail extending deep into the ATP-binding pocket and pushing on the kα3-helix. Comparison of the obtained structure with PI3Kγ-structures of reported selective inhibitors shows that this is a unique feature of this series as none of the reported inhibitors extend as far into the ATP-binding pocket (Figure S1, Supporting Information).

Table 2. PI3K Enzyme and Cell Inhibitory Potencies for 9 and the Matched-Pair Analogue 11[a]

compd	PI3Kγ enz	PI3Kα enz	PI3Kβ enz	PI3Kδ enz	PI3Kγ cell
9	9.2	5.5	4.7	6.7	8.2
11	7.2	7.1[‡]	5.8[‡]	6.6[‡]	<6.0[†]

[a]All biological values are mean of ≥3 replicates except [‡]n = 2, [†]n = 1.

It is important to remember that the crystal structure of **9** is in murine PI3Kδ and thus may not reveal all structural details relevant to understanding the high PI3Kγ selectivity. Compound **9** was profiled in a panel of 132 kinases at 1 μM (Thermo Fisher). Approximately 100% inhibition was observed for PI3Kγ and also for DRAK1, while greater than 50% inhibition was observed for CLK4 and PI3Kδ (Table S1, Supporting Information). The pIC50 values of **9** against DRAK1, and CLK4 were determined and show that even though **9** has a good kinase selectivity profile it is also a potent inhibitor of DRAK1 and CLK4 with pIC50 values of 8.0 and 6.9, respectively. The most potent compounds **8** and **9** did not have a suitable profile for oral administration as they had poor solubility, high in vitro clearance and were very lipophilic. To improve ADME properties, design was focused on reducing lipophilicity. It has been shown that sulfonamides,[6] reversed sulfonamides,[16] and sulfones[17] can be introduced in the ribose pocket of PI3Ks; overlay of the crystal structure of **9** with the public structure of PIK-93 (PDB code 2CHZ),[6] suggested that it could be possible to target the ribose pocket from the isoindolinone core by substitution on the 7-position (Figure 3). This was judged to be a good position to introduce more polar functionalities to decrease lipophilicity. Sulfonamides **12−14**, sulfones **15** and **16**, and reversed sulfonamides **17** and **18**
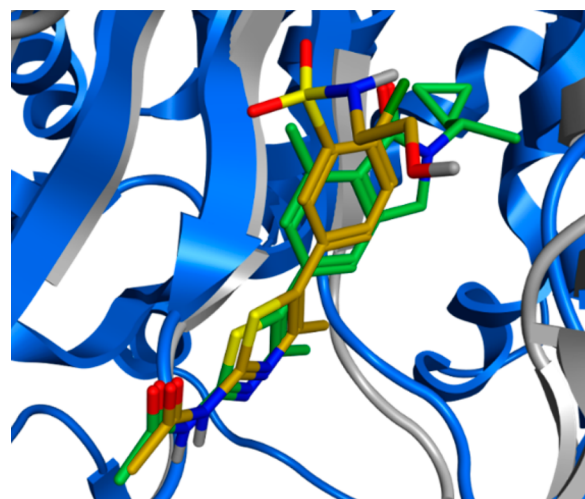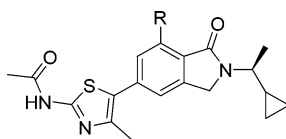

Figure 3. X-ray crystal structure of compound **9** in mouse PI3Kδ (ligand in green, protein in gray, PDB code 6FTN) overlaid with structure of literature compound PIK-93 in PI3Kγ (ligand in yellow, protein in blue, PDB code 2CHZ).[6]

Table 3. Structure, PI3K Enzyme and Cell Inhibitory Potencies, and Pharmacokinetically Relevant Properties of Compounds 12−18[a]

		pIC$_{50}$							
compd	R	PI3Kγ enz	PI3Kα enz	PI3Kβ enz	PI3Kδ enz	PI3Kγ cell	log D, pH 7.4	sol, pH 7.4 (μM)	rat Cl$_{int}$[b]
12	-SO$_2$NH$_2$	9.2	5.2‡	<4.5‡	6.6	7.7‡	2.5	8	<2
13	-SO$_2$NHMe	9.1	5.4	4.6	6.8	8.3	3.0	4	5
14	-SO$_2$NH(CH$_2$)$_2$OMe	8.9	4.9‡	<4.5‡	6.4‡	7.7†	2.7	61	56
15	-SO$_2$Me	9.1	5.1	<4.5	6.5	8.1	2.4	303	<2
16	-SO$_2$(CH$_2$)$_3$OH	8.9	5.1‡	<4.5‡	6.7‡	6.6†	1.9	463	6
17	-NHSO$_2$Me	9.2	5.2‡	4.7‡	6.6	8.6	3.3	<1	4
18	-NHSO$_2$(CH$_2$)$_2$OMe	9.0	5.3‡	4.6‡	6.6‡	8.2†	3.5	14	166

^{a}All biological values are the mean of ≥3 replicates except $^\ddagger n$ = 2, $^\dagger n$ = 1. ^{b}Intrinsic clearance in rat hepatocytes ((μL/min)/10^6 cells).

Table 4. Selected Properties of Compounds 13, 15, and 17

property	13	15	17
PI3Kγ cell pIC$_{50}$	8.3	8.1	8.6
PI3K α/β/δ cell pIC$_{50}$	<4.5/<4.5/6.4	<4.5/<4.5/6.0	<4.5/<4.5/6.1
aq solubility pH 6.5 (μM)	9	111	5
hERG pIC$_{50}$	<4.5	4.5	4.7
cytotoxicity THP1 pIC$_{50}$	3.8	4.1	4.7
mitochondrial toxicity	not active	not active	not active
PPB human/rat/dog (% free)	9/8/10	12/12/22	1/1/5
hepatocyte Cl$_{int}$ human/rat/dog ((μL/min)/10^6 cells)	0.5/4.5/2.1	0.4/1.7/1.0	3.4/3.7/7.6
in vivo PK			
rat Cl ((mL/min)/kg), $t_{1/2}$ (h), F (%), V_{ss} (L/kg)	4.4, 2.6, 30, 1.0	6.3, 2.3, 51, 1.2	0.7, 6.7, 49, 0.4
dog Cl ((mL/min)/kg), $t_{1/2}$ (h), F (%), V_{ss} (L/kg)	2.1, 12, 44, 2.2	3.3, 3.9, 82, 1.1	6.2, 1.3, 1.6, 0.7

extending from the 7-position of the isoindolinone core were prepared. The majority of these compounds had maintained or increased PI3Kγ potency while at the same time having a lower log D (Table 3). The most potent compounds in the enzymatic and cellular assay were N-methylsulfonamide 13, methyl sulfone 15, and reversed methylsulfonamides 17 and 18. Compound 18, however, exhibited high intrinsic clearance in rat hepatocytes. Compounds 13, 15, and 17 were selected for further profiling.

All the shortlisted compounds, 13, 15, and 17, showed excellent isoform selectivity in the biochemical assays, and this profile was also confirmed in mechanism-based cellular assays measuring phosphorylation of AKT. The compounds showed high activity in the PI3Kγ target engagement cell assay and >100-fold selectivity in a human Jeko-1B cell line that assesses PI3Kδ activity (Table 4). The compounds were inactive in two other cell assays: a human MDA MB-468 cell line and a human BT4 cell line that assess activity of PI3Kα and PI3Kβ, respectively. Compound 15 had considerably better kinetic solubility than 13 and 17 (Table 3). The difference was less pronounced when thermodynamic solubility at pH 6.5 was measured, but 15 was still the most soluble (Table 4). The compounds had a clear margin against inhibition of the hERG channel and also for general cytotoxicity assessed in THP1 cells and HepG2 cells. In vitro PK data of the three compounds showed that 15 consistently had the lowest intrinsic clearance and highest free fraction across three species (human, rat, and dog). In vivo, 17 showed low clearance in rat and had the longest half-life of the shortlisted compounds in this species.

Also in dog, 17 had a lower clearance than predicted from in vitro data, but in this species in vivo clearance was the highest among the three compounds. In addition, bioavailability of 17 in dog was only 1.6%. Compound 15 on the other hand had good bioavailability and low clearance in both species which was consistent with in vitro data. On the basis of these data, 15 was identified as the compound with the best profile for oral administration and was chosen for further profiling. Kinase selectivity profiling of 15 at 1 μM in a panel of 395 kinases (Thermo Fisher) including protein and lipid kinases showed excellent kinase selectivity (Table S2, Supporting Information), and no activity could be detected for the previously observed off-targets DRAK1 and CLK4.

Except for PI3Kγ (95%) and -δ (66%) the only kinases that showed greater than 50% inhibition at 1 μM were the class II PI3Ks: PI3KC2β (84%) and PI3KC2γ (71%). Thus, to get a more complete view of the selectivity toward class II and class III PI3Ks, pIC$_{50}$ values of 15 against all class II and class III PI3Ks were determined (Table 5). These data showed that 15

Table 5. Selectivity Profiling of Compound 15 toward Class II and Class III PI3Ks[a]

pIC$_{50}$				
PI3Kγ enz	PI3KC2α enz	PI3KC2β enz	PI3KC2γ enz	PI3KC3 enz
>9.2^b	<5	7.5	5.5	5.1

^{a}All biological values are the mean of ≥2 replicates. ^{b}The exact pIC$_{50}$ could not be determined in this assay format.

inhibits the class II PI3K PI3KC2β with a pIC$_{50}$ of 7.5 as compared to a pIC$_{50}$ > 9.2 for PI3Kγ in a comparable biochemical assay. Relatively little is known about the role of class II PI3Ks,[18] and no notable activity of **15** was recorded for the other class II and class III PI3Ks.

Compound **15** was also screened in a wide ligand profile screen (CEREP), covering 89 distinct molecular targets (Table S4, Supporting Information). Compound **15** showed good selectivity margins, with only one target, P2Y$_1$, with a K_i below 1 μM. Follow-up screening showed no activity (<100 μM) of **15** as agonist or antagonist in whole cell P2Y$_1$ assays. On the basis of the encouraging pharmacokinetic and safety/selectivity profile of **15**, we decided to progress into a rat LPS-induced acute inflammation model, measuring airway neutrophilia. Compound **15** was dosed 2 h prior to challenge and inhibited neutrophil migration with a dose-response over doses of 0.1, 0.5, and 2.5 mg/kg (Figure 4). These data strongly suggest that oral administration of **15** inhibits PI3Kγ function in vivo.
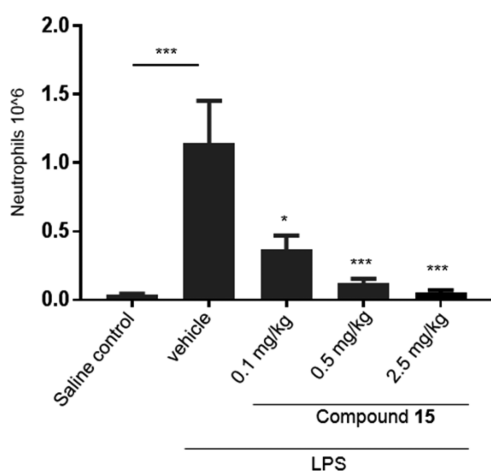

Figure 4. Effect of compound **15** on LPS-induced neutrophil migration in rats. LPS challenged Wistar females were dosed po with **15** 2 h prior to challenge. 4 h after challenge the animals were sacrificed. Lung fluid was collected by lavage, and differential cell count was performed using a SYSMEX XT-1800i. Neutrophil migration was significantly inhibited in a dose-dependent manner with **15**. $n = 8$ in all groups ($n = 10$ for vehicle group). Statistical significance is indicated as follows above the columns: (∗) $p < 0.001$; (∗∗∗) $p < 0.05$.

Compound **15** was prepared in four steps starting from a methylester derivative that was reacted with (S)-1-cyclopropyl-ethanamine to give isoindolinone **19** (Scheme 1). The aminothiazole was introduced by a Pd-catalyzed coupling of isoindolinone **19** with N-(4-methylthiazol-2-yl)acetamide. This was followed by an S$_N$Ar reaction with sodium methanthiolate

to give the intermediate sulfide which could be oxidized to the desired sulfone **15** by using m-CPBA.

■ CONCLUSION

A series of highly isoform-selective PI3Kγ inhibitors have been developed starting from a high quality HTS hit. This series, which contains an alkyl-substituted isoindolinone core, exhibits remarkable isoform selectivity which originates from the N-alkyl tail extending deep into the ATP-binding pocket. The initial hit was efficiently progressed by use of structure based design to more advanced compounds, e.g., **15**. This compound combines high biochemical and cellular potency with excellent isoform selectivity and has an attractive pharmacokinetic and in vitro safety profile. Oral administration of **15** resulted in a dose-dependent inhibition of LPS-induced airway neutrophilia in rats.

■ EXPERIMENTAL SECTION

All compounds were purified to ≥95% purity (HPLC). Further synthetic details and full descriptions of biological methods are contained in the Supporting Information.

N-(5-{7-Chloro-2-[(1S)-1-cyclopropylethyl]-1-oxo-2,3-dihydro-1H-isoindol-5-yl}-4-methyl-1,3-thiazol-2-yl)acetamide (8). Cs$_2$CO$_3$ (37.3 g, 114 mmol) was added to a flask containing **19** (18.0 g, 57 mmol), N-(4-methyl-1,3-thiazol-2-yl)acetamide (10.7 g, 69 mmol), tri-tert-butylphosphonium tetrafluoroborate (3.3 g, 11 mmol), and Pd(OAc)$_2$ (1.3 g, 6 mmol) in DMF (300 mL). The resulting mixture was heated at 100 °C. After 2 h it was cooled to rt, filtered through Celite, and concentrated. The residue was chromatographed (silica gel; 0−25% of MeOH in DCM) to afford the title compound (14.0 g, 63%) as a yellow solid. ^{1}H NMR (500 MHz, DMSO-d_6) δ 0.2−0.27 (m, 1H), 0.35−0.43 (m, 2H), 0.52−0.61 (m, 1H), 1.08−1.14 (m, 1H), 1.28 (d, J = 6.8 Hz, 3H), 2.16 (s, 3H), 2.40 (s, 3H), 3.52−3.63 (m, 1H), 4.56 (s, 2H), 7.50 (s, 1H), 7.64 (s, 1H), 12.23 (s, 1H). HRMS: m/z calcd 390.1043, found 390.1022.

N-(5-{2-[(1S)-1-Cyclopropylethyl]-7-(methylsulfonyl)-1-oxo-2,3-dihydro-1H-isoindol-5-yl}-4-methyl-1,3-thiazol-2-yl)-acetamide (15). Sodium methanethiolate (5.0 g, 71 mmol) was added to **8** in DMF (80 mL). The resulting mixture was heated at 110 °C for 2 h. The solvent was removed under reduced pressure, and the reaction mixture was poured into water. The resulting precipitate was collected by filtration, washed with water (200 mL) and EtOAc (50 mL), and dried under vacuum to afford the intermediate sulfide (4.10 g, 72%), which was used in the next step (below) without further purification.

m-CPBA (3.3 g, 19.3 mmol) was added to the sulfide prepared above (3.1 g, 7.7 mmol) in DCM (120 mL). The resulting mixture was stirred at 0 °C for 1 h, then warmed to rt and stirred for 1 h. The reaction mixture was quenched with saturated NaHCO$_3$ (200 mL) and extracted with DCM. The organic layer was dried over Na$_2$SO$_4$, filtered, and concentrated. The crude product was purified by preparative HPLC to afford the title compound **15** (1.2 g, 36%) as a white solid. ^{1}H NMR (500 MHz, DMSO-d_6) δ 0.24−0.29 (m, 1H), 0.38−0.46 (m, 2H), 0.57−0.62 (m, 1H), 1.11−1.19 (m, 1H), 1.31 (d, J = 6.8 Hz, 3H), 2.17 (s, 3H), 2.44 (s, 3H), 3.59−3.65 (m, 4H), 4.70 (s,

Scheme 1. Synthesis of Compound 15[a]
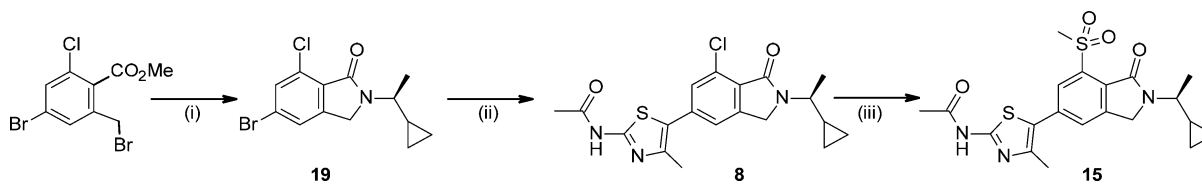
[a]Reagents and conditions: (i) (S)-1-cyclopropylethanamine, B(OH)$_3$, K$_2$CO$_3$, MeCN, 80 °C, 34%; (ii) N-(4-methylthiazol-2-yl)acetamide, Pd(OAc)$_2$, [(t-Bu)$_3$PH]BF$_4$, Cs$_2$CO$_3$, DMF, 100 °C, 63%; (iii) (a) NaSMe, DMF, 110 °C, 72%, (b) m-CPBA, DCM, 0 °C, 36%.

2H), 8.00 (d, J = 1.5 Hz, 1H), 8.05 (d, J = 1.5 Hz, 1H), 12.30 (s, 1H). ^{13}C NMR (126 MHz, DMSO-d_6) δ 3.4, 3.9, 15.5, 16.3, 18.0, 22.5, 43.1, 45.9, 52.1, 121.8, 126.6, 127.3, 127.7, 135.4, 137.7, 144.6, 145.9, 156.3, 163.6, 168.7. [α]$_D$ +60 (c 1 g/100 mL, MeCN, 20 °C). HRMS: m/z calcd 434.1208, found 434.1201.

5-Bromo-7-chloro-2-[(1S)-1-cyclopropylethyl]-2,3-dihydro-1H-isoindol-1-one (19). (S)-1-Cyclopropylethanamine (2.4 mL, 23 mmol) was added to a flask containing methyl 4-bromo-2-(bromomethyl)-6-chlorobenzoate (7.8 g, 23 mmol) in acetonitrile (80 mL). Boric acid (1.4 g, 23 mmol) was added, followed by portionwise addition of K_2CO_3 (6.3 g, 46 mmol) over 2 min. The mixture was allowed to stir at rt overnight. The reaction mixture was filtered and washed with acetonitrile. The combined acetonitrile filtrates were concentrated and the residue was chromatographed (silica gel; 5−30% of EtOAc in heptane) to afford the title compound (2.4 g, 34%) as a pink solid. ^{1}H NMR (500 MHz, DMSO-d_6) δ 0.15−0.26 (m, 1H), 0.32−0.45 (m, 2H), 0.51−0.61 (m, 1H), 1.06−1.14 (m, 1H), 1.26 (d, J = 6.8 Hz, 3H), 3.48−3.58 (m, 1H), 4.52 (s, 2H), 7.76 (d, J = 1.3 Hz, 1H), 7.84 (d, J = 1.3 Hz, 1H). m/z (ESI) 316 [M + H]$^+$.

■ ASSOCIATED CONTENT

ⓢ Supporting Information

The Supporting Information is available free of charge on the ACS Publications website at DOI: 10.1021/acs.jmed-chem.8b00447.

> Experimental procedures and spectroscopic data for final compounds and detailed pharmacology methods (PDF)
> Molecular formula strings and some data (CSV)

Accession Codes

The crystal structure for compound **9** (PDB code 6FTN) has been deposited with the Protein Data Bank. The authors will release coordinates and experimental data upon publication.

■ AUTHOR INFORMATION

Corresponding Authors

*N.P.: phone, +46 31 7761498; e-mail, nils.pemberton@astrazeneca.com.

*M.M.: phone, +46 31 7064830; e-mail, mickael.mogemark@astrazeneca.com.

ORCID ⓘ

Nils Pemberton: 0000-0002-8875-7221
Cristina Gardelli: 0000-0003-1169-2180
Matthew W. D. Perry: 0000-0002-9799-0746

Present Addresses

#N.S.H.: University of Lincoln, Brayford Pool, Lincoln, Lincolnshire LN6 7TS, U.K.

∇K.K.: Bioglan AB, P.O. Box 50310, 202 13 Malmö, Sweden.

○J. K.: Cobra Biologics, Gärtunavägen 10, 152 57 Södertälje, Sweden.

◆M.T.: Boehringer-Ingelheim Pharma, Birkendorf Strasse, Biberach 88397, Germany.

Notes

The authors declare no competing financial interest.

■ ABBREVIATIONS USED

CLK, CDC-like kinase; DRAK, DAPK-related apoptosis-inducing kinase; LPS, lipopolysaccharide; PI3, phosphoinositide 3-kinase

■ REFERENCES

(1) Sapey, E.; Greenwood, H.; Walton, G.; Mann, E.; Love, A.; Aaronson, N.; Insall, R. H.; Stockley, R. A.; Lord, J. M. Phosphoinositide 3-kinase inhibition restores neutrophil accuracy in the elderly: toward targeted treatments for immunosenescence. *Blood* **2014**, *123*, 239−248.

(2) Sasaki, T.; Irie-Sasaki, J.; Jones, R. G.; Oliveira-dos-Santos, A. J.; Stanford, W. L.; Bolon, B.; Wakeham, A.; Itie, A.; Bouchard, D.; Kozieradzki, I.; Joza, N.; Mak, T. W.; Ohashi, P. S.; Suzuki, A.; Penninger, J. M. Function of PI3Kγ in thymocyte development, T cell activation, and neutrophil migration. *Science* **2000**, *287*, 1040−1046.

(3) Cushing, T. D.; Metz, D. P.; Whittington, D. A.; McGee, L. R. PI3Kδ and PI3Kγ as targets for autoimmune and inflammatory diseases. *J. Med. Chem.* **2012**, *55*, 8559−8581.

(4) Ruckle, T.; Schwarz, M. K.; Rommel, C. PI3Kγ inhibition: towards an "aspirin of the 21st century"? *Nat. Rev. Drug Discovery* **2006**, *5*, 903−918.

(5) Stark, A. K.; Sriskantharajah, S.; Hessel, E. M.; Okkenhaug, K. PI3K inhibitors in inflammation, autoimmunity and cancer. *Curr. Opin. Pharmacol.* **2015**, *23*, 82−91.

(6) Knight, Z. A.; Gonzalez, B.; Feldman, M. E.; Zunder, E. R.; Goldenberg, D. D.; Williams, O.; Loewith, R.; Stokoe, D.; Balla, A.; Toth, B.; Balla, T.; Weiss, W. A.; Williams, R. L.; Shokat, K. M. A pharmacological map of the PI3-K family defines a role for p110α in insulin signaling. *Cell* **2006**, *125*, 733−747.

(7) Bi, L.; Okabe, I.; Bernard, D. J.; Nussbaum, R. L. Early embryonic lethality in mice deficient in the p110β catalytic subunit of PI 3-kinase. *Mamm. Genome* **2002**, *13*, 169−172.

(8) Bi, L.; Okabe, I.; Bernard, D. J.; Wynshaw-Boris, A.; Nussbaum, R. L. Proliferative defect and embryonic lethality in mice homozygous for a deletion in the p110α subunit of phosphoinositide 3-kinase. *J. Biol. Chem.* **1999**, *274*, 10963−10968.

(9) Evans, C. A.; Liu, T.; Lescarbeau, A.; Nair, S. J.; Grenier, L.; Pradeilles, J. A.; Glenadel, Q.; Tibbitts, T.; Rowley, A. M.; DiNitto, J. P.; Brophy, E. E.; O'Hearn, E. L.; Ali, J. A.; Winkler, D. G.; Goldstein, S. I.; O'Hearn, P.; Martin, C. M.; Hoyt, J. G.; Soglia, J. R.; Cheung, C.; Pink, M. M.; Proctor, J. L.; Palombella, V. J.; Tremblay, M. R.; Castro, A. C. Discovery of a selective phosphoinositide-3-kinase (PI3K)-γ Inhibitor (IPI-549) as an immuno-oncology clinical candidate. *ACS Med. Chem. Lett.* **2016**, *7*, 862−867.

(10) Kaneda, M. M.; Messer, K. S.; Ralainirina, N.; Li, H.; Leem, C. J.; Gorjestani, S.; Woo, G.; Nguyen, A. V.; Figueiredo, C. C.; Foubert, P.; Schmid, M. C.; Pink, M.; Winkler, D. G.; Rausch, M.; Palombella, V. J.; Kutok, J.; McGovern, K.; Frazer, K. A.; Wu, X.; Karin, M.; Sasik, R.; Cohen, E. E.; Varner, J. A. PI3Kγ is a molecular switch that controls immune suppression. *Nature* **2016**, *539*, 437−442.

(11) Collier, P. N.; Messersmith, D.; Le Tiran, A.; Bandarage, U. K.; Boucher, C.; Come, J.; Cottrell, K. M.; Damagnez, V.; Doran, J. D.; Griffith, J. P.; Khare-Pandit, S.; Krueger, E. B.; Ledeboer, M. W.; Ledford, B.; Liao, Y.; Mahajan, S.; Moody, C. S.; Roday, S.; Wang, T.; Xu, J.; Aronov, A. M. Discovery of highly isoform selective thiazolopiperidine inhibitors of phosphoinositide 3-kinase γ. *J. Med. Chem.* **2015**, *58*, 5684−5688.

(12) Full experimental details of biochemical assays (α, β, γ, and δ) and PI3Kγ target engagement cellular assays are included in the Supporting Information.

(13) By May 2018 the RSCB PDB contains 77 crystal structures of human PI3Kγ.

(14) Bruce, I.; Akhlaq, M.; Bloomfield, G. C.; Budd, E.; Cox, B.; Cuenoud, B.; Finan, P.; Gedeck, P.; Hatto, J.; Hayler, J. F.; Head, D.; Keller, T.; Kirman, L.; Leblanc, C.; Le Grand, D.; McCarthy, C.; O'Connor, D.; Owen, C.; Oza, M. S.; Pilgrim, G.; Press, N. E.; Sviridenko, L.; Whitehead, L. Development of isoform selective PI3-kinase inhibitors as pharmacological tools for elucidating the PI3K pathway. *Bioorg. Med. Chem. Lett.* **2012**, *22*, 5445−5450.

(15) Leahy, J. W.; Buhr, C. A.; Johnson, H. W.; Kim, B. G.; Baik, T.; Cannoy, J.; Forsyth, T. P.; Jeong, J. W.; Lee, M. S.; Ma, S.; Noson, K.; Wang, L.; Williams, M.; Nuss, J. M.; Brooks, E.; Foster, P.; Goon, L.; Heald, N.; Holst, C.; Jaeger, C.; Lam, S.; Lougheed, J.; Nguyen, L.; Plonowski, A.; Song, J.; Stout, T.; Wu, X.; Yakes, M. F.; Yu, P.; Zhang, W.; Lamb, P.; Raeber, O. Discovery of a novel series of potent and

orally bioavailable phosphoinositide 3-kinase γ inhibitors. *J. Med. Chem.* **2012**, *55*, 5467−5482.

(16) D'Angelo, N. D.; Kim, T. S.; Andrews, K.; Booker, S. K.; Caenepeel, S.; Chen, K.; D'Amico, D.; Freeman, D.; Jiang, J.; Liu, L.; McCarter, J. D.; San Miguel, T.; Mullady, E. L.; Schrag, M.; Subramanian, R.; Tang, J.; Wahl, R. C.; Wang, L.; Whittington, D. A.; Wu, T.; Xi, N.; Xu, Y.; Yakowec, P.; Yang, K.; Zalameda, L. P.; Zhang, N.; Hughes, P.; Norman, M. H. Discovery and optimization of a series of benzothiazole phosphoinositide 3-kinase (PI3K)/mammalian target of rapamycin (mTOR) dual inhibitors. *J. Med. Chem.* **2011**, *54*, 1789−1811.

(17) Bergamini, G.; Bell, K.; Shimamura, S.; Werner, T.; Cansfield, A.; Muller, K.; Perrin, J.; Rau, C.; Ellard, K.; Hopf, C.; Doce, C.; Leggate, D.; Mangano, R.; Mathieson, T.; O'Mahony, A.; Plavec, I.; Rharbaoui, F.; Reinhard, F.; Savitski, M. M.; Ramsden, N.; Hirsch, E.; Drewes, G.; Rausch, O.; Bantscheff, M.; Neubauer, G. A selective inhibitor reveals PI3Kγ dependence of T(H)17 cell differentiation. *Nat. Chem. Biol.* **2012**, *8*, 576−82.

(18) Falasca, M.; Hamilton, J. R.; Selvadurai, M.; Sundaram, K.; Adamska, A.; Thompson, P. E. Class II phosphoinositide 3-kinases as novel drug targets. *J. Med. Chem.* **2017**, *60*, 47−65.